Morphology of patterned semiconductor III-V surfaces prepared by spontaneous anisotropic chemical etching

José-Guadalupe Bañuelos[1], Elena V. Basiuk[2,*] and José-Manuel Saniger-Blesa[3]
Centro de Ciencias Aplicadas y Desarrollo Tecnológico, Universidad Nacional Autónoma de México, México, D.F.
[1]*gpeban@aleph.cinstrum.unam.mx*, [2]*elenagd@servidor.unam.mx*, [3]*saniger@aleph.cinstrum.unam.mx*

Recibido el 30 de abril de 2002; aceptado el 18 de marzo de 2003

In the present paper we report on scanning electron microscopy and atomic force microscopy study of different microreliefs obtained through a spontaneous anisotropic etching (that is without the use of masking, photochemical and photoelectrochemical techniques) of the surfaces of monocrystalline $A^{III}B^{V}$-type semiconductors: InP(100) doped with S and Fe, GaP(100), GaSb(100), InSb(100) and GaAs(100). The microrelief morphology (star-like, pyramides, grooves, etc.) depends on acidic etchant employed. Estimation of the activation energy demonstrates that the etching with microrelief formation occurs in the kinetic region. The most interesting InP microrelief is the two-dimensional groove-shaped one, which might be suitable to produce antireflection surfaces for solar cells. The conditions have been optimized to fabricate this microrelief with a given groove period of 0.6 to 3.7 μm. Morphology of different textured surfaces of other $A^{III}B^{V}$ semiconductors is also discussed.

Keywords: AFM; SEM; microreliefs; anisotropic etching; textured surfaces; $A^{III}B^{V}$ semiconductors.

En el artículo se presenta un estudio por microscopía electrónica de barrido y microscopía de fuerza atómica de diferentes microrrelieves obtenidos por grabado (o ataque) químico anisótropo espontáneo (es decir, sin usar mascarillas ni técnicas fotoquímicas y fotoelectroquímicas) en superficies de semicoductores monocristalinos miembros del grupo de los semiconductores $A^{III}B^{V}$: InP(100) dopado por S y Fe, GaP(100), GaSb(100), InSb(100) y GaAs(100). La forma del microrrelieve (canales, estrellas, pirámides, etc.) depende del agente ácido empleado. La estimación de la energía de activación del proceso pone de manifiesto que la formación de microrrelieves ocurre en la región cinética. Los relieves generados en InP con forma de microcanales bidimensionales son de especial interés por su posible aplicación como superficies antirreflejantes en la fabricación de celdas solares. La optimización de las condiciones de grabado en InP permite producir microcanales con periodos espaciales en un intervalo de 0.6 a 3.7 μm. También se discuten las morfologías de otros tipos obtenidos de superficies de semiconductores $A^{III}B^{V}$ texturizadas.

Descriptores: AFM; SEM; microrelieves; ataque anisótropo; superficies texturizadas; semiconductores $A^{III}B^{V}$.

PACS: 68.35.Bs; 68.37.P; 81.65.C

1. Introduction

The anisotropic etching phenomenon (the dependence of etching rate on crystal orientation) can be used for the formation of two and three-dimensional structures on semiconductor surfaces, and thus it is of great interest for the technology of semiconductor photoelectric and optical devices, such as solar cells, diffraction gratings, and laser diodes [1-11]. Patterning of GaAs, InP semiconductor substrates and their heterostructure overgrowth has a great potential for creating new semiconductor micro- and nanostructures grown on U-, and V-groove substrates. In the future, the use of InP and GaP-based materials is expected to appear more advantageous than classical silicon for some specific application, such as the development of quantum wire lasers emitting in the wavelength range of 1.3 to 1.6 μm [9]. Indium antimonide (InSb) well matches the mid-infrared atmosferic transmission window (3-5 μm) and, consequently, it is the primary material for mid-IR focal plane arrays. At longer wavelengths, specifically to access the 8-12 μm, the materials available are limited to GaSb [14]. In addition, InSb is a compound with the highest room-temperature electron mobility of any known solid; magneto-resistors made of it have extremely high sensitivity at magnetic fields higher than 0.1 T. [15]. Such narrow-bandgap semiconductors have attracted a lot of attention because of their potential applications in infrared sensors and high-speed devices. During their fabrication process, some special etchants are used [16]. An attractive method for decreasing surface reflectivity, specifically in solar cell fabrication, is the surface texturation, due to the transformation of semiconductor into a light trap. Besides, it was reported that the formation of metal-semiconductor interface on the base of such textured surfaces leads to increasing the photocurrent of surface-barrier structure by several times. It is very important to be able to vary the type and geometric parameters of such surface microrelief morphology without worsening of their electrical and recombination parameters. The advantage of anisotropic etching is the creation of a controlled geometry without formation of damaged surface layer [7-10]. That is why further development of anisotropic wet chemical etching processes for fabrication of micro- and nanoscale structures in InP and GaP, with predetermined etching profile, is of great importance. A detailed knowledge of the semiconductor behavior in different etchants plays a key role in this research.

In the present work we report on a spontaneous anisotropic etching (that is without the use of masking, photochemical or photoelectrochemical etching techniques) of the surfaces of InP(100) doped with Fe and S atoms, GaP(100), InSb(100), GaSb(100) and GaAs(100) in diferent etchants, and on scanning electron microscopy (SEM) and atomic force microscopy (AFM) study of the resulting microreliefs.

2. Experimental

The specimens were cut from semiconductor wafers commercially available from Atomergic Chemetals Corporation: N-type InP(100), S doped, with carrier concentration n=2.6$\times 10^{16}$ cm^{-3}; Semi Insulating-type InP(100), Fe doped, resistivity $> 10^7$ Ohm cm; P-type GaP(100), Zn doped, with carrier concentration n=1-2$\times 10^{18}$ cm^{-3}; N-type InSb(100), Te doped, with carrier concentration n=3-5$\times 10^{17}$ cm^{-3}; N-type GaSb(100), Te doped, with carrier concentration n=6-8$\times 10^{17}$ cm^{-3}; and N-type GaAs(100), with carrier concentration n=1-5$\times 10^{17}$ cm^{-3}. Prior to the experiments, the specimens were cleaned by boiling in carbon tetrachloride and acetone, then rinsed in deionized water. Concentrated analytical grade inorganic acids were used for preparation of anisotropic etchants. The etching was carried out in a 150 ml cylindrical quartz reactor. Etching behavior and surface morphology were examined by a direct observation of pattern evolution, by means of of high-resolution scanning electron microscopy (SEM) and atomic force microscopy (AFM). AFM measurements were performed using an AutoProbe CP instrument from Park Scientific Instruments (tapping mode; cantilever typical force constant of 3.2 N/m; typical resonance frequency of 90 kHz). For SEM measurements, a JEOL JSM 5200 instrument was used (operating at 15-25 kV; maximum resolution of 5.5 nm).

3. Results and discussion

The anisotropic chemical etching of InP(100) surfaces (doped with S atoms) in concentrated hydrochloric acid leads to the formation of approximately parallel grooves oriented along [011] direction. The groove orientation appears to be orthogonal at the parallel planes (100) and ($\bar{1}00$) due to the $\langle 111 \rangle$ crystallografic polarity of zincblende-type crystal [3,5,7]. The grooves formed have a sawtooth profile (Fig. 1a,b). The inclined planes form an angle of 25 $^\circ$ with respect to the (100) surfaces and correspond to In $\{311\}$ crystallographic planes. Increasing the etching duration from 0.5 to 6 min causes an increase in period of the obtained grating from 0.6 to 3.7 μm. The depth of the grooves does not undergo evident change and remains about 0.14 μm. The geometrical parameters of these grooves are highly reproducible. This microrelief surface has In enrichment, as confirmed with Auger electron spectroscopy [12].

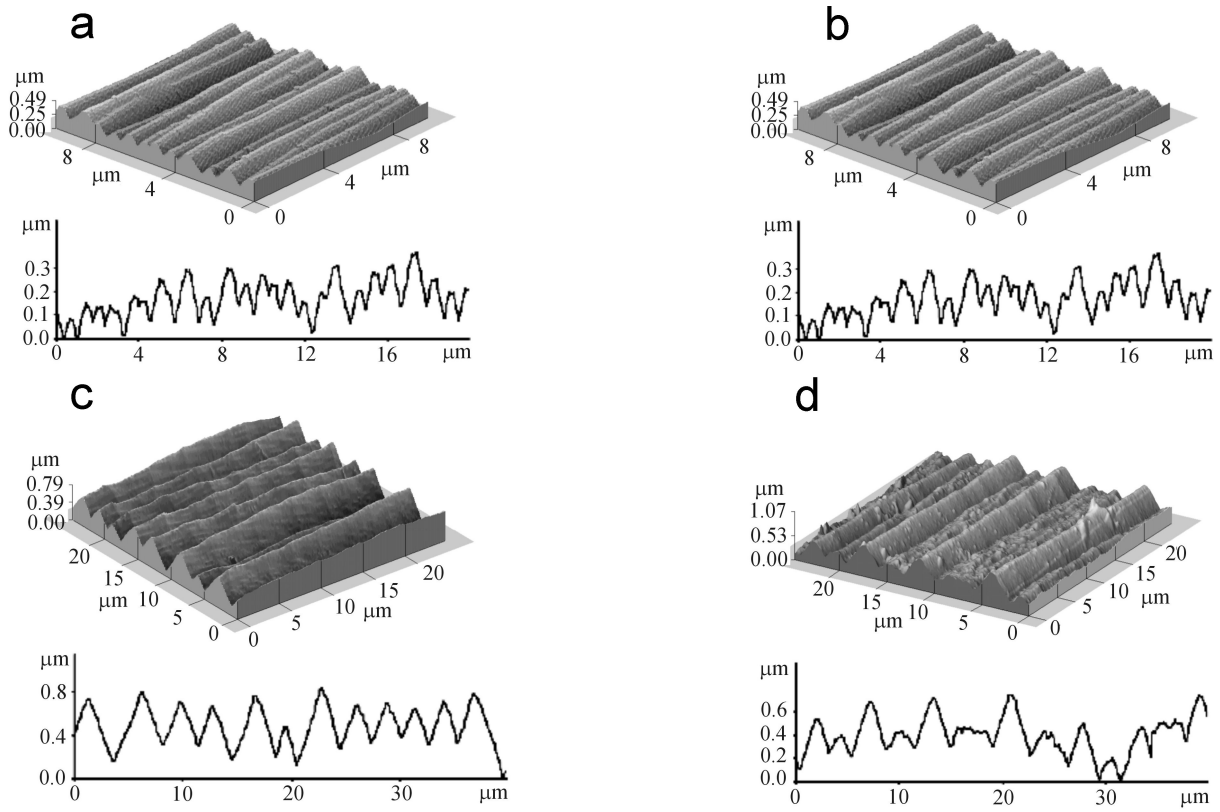

FIGURE 1. AFM images and geometrical parameters of surface microreliefs at: (a) InP(100) and (b) InP($\bar{1}00$) etched in concentrated HCl at 25 $^\circ$ C for 1 min; (c) InP(100) and (d) InP($\bar{1}00$) etched in $10H_3PO_4$:$10H_2SO_4$:$1K_2S_2O_8$:$5H_2O$ at 70 $^\circ$ C for 3 min.

A very similar morphology (parallel grooves) of the same InP surface was obtained in a multicomponent etchant, with the composition of $10H_3PO_4$:$10H_2SO_4$:$1K_2S_2O_8$:$5H_20$ (Fig. 1c). In this case V-grooves formed only on one side of InP(100) surface. Their inclined planes form an angle of 15˚-17˚ with respect to the (100) surface, and the most probable planes deduced from this angle are $\{511\}$ planes. The other etched side of InP(100) surface had wide mesa-shaped-grooves with undesirable roughness (Fig. 1d). Their inclined planes also are $\{511\}$ planes. The period of the groove-like microrelief shown in Fig. 1c varies within 0.7 to 3.4 μm, and the depth is of about 0.42 μm. This patterned surface also has an In-enrichment pointed out from Auger spectroscopy scanning [12].

The InP samples doped with Fe atoms (semi-insulators) exhibited a poorer quality of textured surfaces in HCl etchant. The formed grooves are short, neither periodic nor parallel, and with many roughnesses on their planes (Fig. 2a). We found another route to improve microrelief quality, through a two-step etching procedure: first, etching in $1HNO_3$:1HCl mixture, which eliminated most surface imperfections; and then anisotropic etching in HCl. The improvement of this microrelief surface es evident from Fig. 2b, where the obtained grooves are highly parallel and periodic, as well as without noticeable roughnesses. The depth of the grooves does not undergo evident change and remains about 0.3 μm for both routes. Thus, the influence of the impurities on the microrelief morphology and the quality of patterning can be clearly seen: S-InP and Fe-InP have different carrier concentration, where S-InP is a n-type semiconductor, and Fe-InP is a semi-insulator.

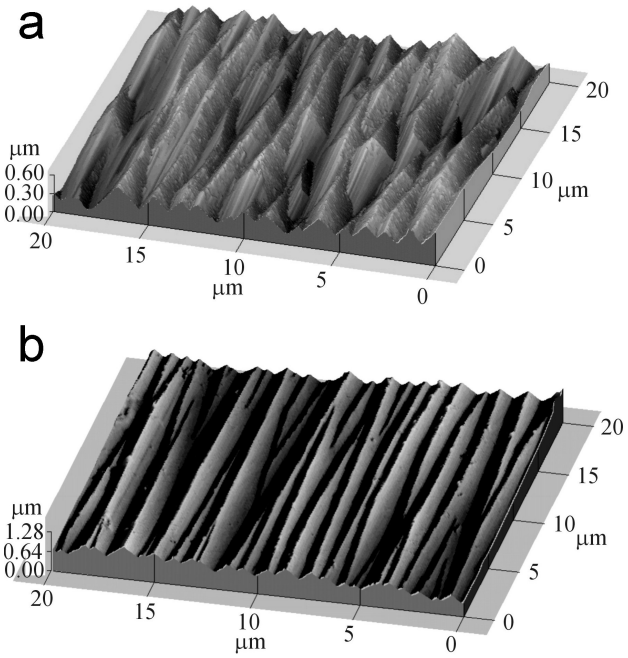

FIGURE 2. AFM images of InP(100) (dopated by atoms of Fe) surface after: (a) etching in concentrated HCl at 25 ˚C for 1 min; (b) two-step anisotropic etching in $1HNO_3$:1HCl, followed by HCl.

The process of semiconductor dissolution is very complicated and sensitive also to changes in etching conditions. Adding $FeCl_3$ to concentrated HCl changes the morphology discussed above by shortening the grooves, and in $FeCl_3$/HCl solution with a higher $FeCl_3$ concentration, "hachures" (parallel short strokes) oriented in [011] direction formed.

In addition to the grooves, a few other microreliefs have been obtained on InP surfaces. For example, etching in mixture $1H_2SO_4$:1HCl mixture results in formation of a "parquet" microrelief, which consists of truncated tetrahedral pyramids. The largest In enrichment for this microrelief surface studied by Auger spectroscopy occures at up to 50 Å-depth [12]. For concentrated H_2SO_4, at the earliest stages of etching, convex rounded figures form, which then evolve into star-like structures (Fig. 3a). Etching in the same acid (but at lower temperatures) causes the formation of big layered "knobs" (Fig. 3b), combining a rounded shape and the tendency to a multitipped skeletone structure. It was observed that spacings between microrelief figures depend of the tratements conditions in every case.

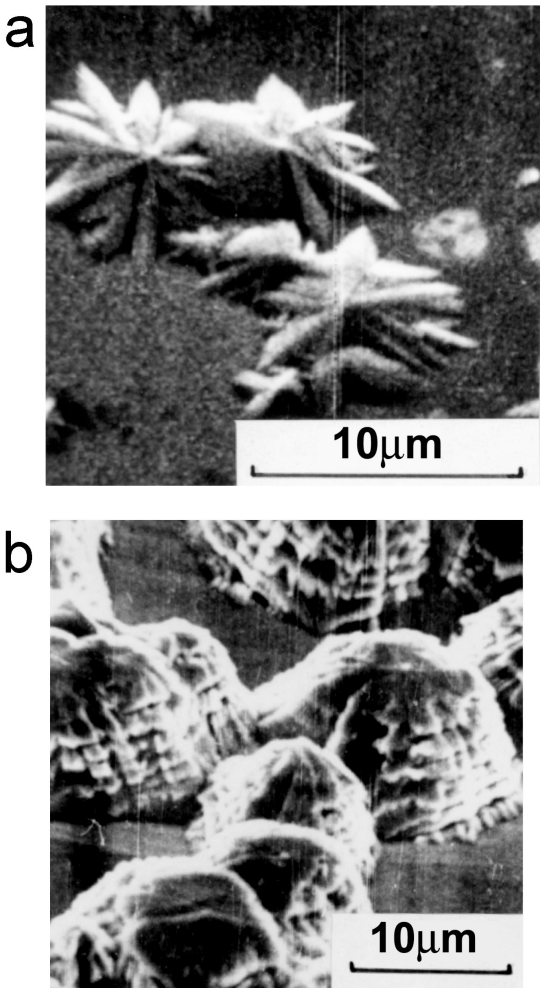

FIGURE 3. SEM microphotographs of the InP(100) surfaces after anisotropic etching in: (a) concentrated H_2SO_4 at 105 ˚C for 3 min; (b) concentrated H_2SO_4 at 90 ˚C for 7 min.

For GaP(100) surfaces, it was found that concentrated H_3PO_4 exhibits selective etching properties, producing grooves also elongated in [011] direction (Fig. 4d), similarly to the InP grating-like microrelief. The grooves on the (100) surface are perpendicular to those on the $(\bar{1}00)$ surface. The formation of this microrelief was observed during 10 min of etching. After 1 min, rectangular pits of mesa-shape profile and of apparent 0.1-μm depth were found to emerge at several places (Fig. 4a). Their long and short sides are oriented in [011] and $[01\bar{1}]$ directions, respectively. Subsequent H_3PO_4 treatment for 2 min extended these pits in length as well as in depth, and after treatment for 3 min they started to "melt" together forming a net-like structure shown in Fig. 4d. The orientation of these grooves along [011] direction implies that this surface morphology is also closely related to GaP crystallographic properties, similarly to the case of InP. Crystallographic (511) close packed planes of Ga act as an inhibitory planes for the etching and determine the overall etch rate. As a result, an overwhelming majority of the grooves are oriented in a [011] direction and the hill-side face should be mainly represented by Ga(111) plane.

A variety of concentrated H_3PO_4-based anisotropic etchants produce essentially similar morphologies. The one worth mentioning is a very interesting case of surface microrelief on GaP(100) revealed by a two-step treatment: first in concentrated HCl, then in concentrated H_3PO_4 (Fig. 5), where a concave pyramidal microrelief forms, filling the surfaces completely and uniformly. The apparent microrelief height is 0.2-0.5 μm.

It was reported earlier that such textured InP surfaces can be used for decreasing surface reflectivity, particularly in solar cell fabrication. Also it was shown that this method of InP surfaces patterning is a promising way to increase photodetector responsivity in visible, near infrared and ultraviolet spectral range without worsening electrical and recombination parameters of the interface [8-11]. Bearing in mind the suitability for fabrication antireflection surfaces for solar cells, it was important in our study to find similar textures (groove-type, grating-like, etc.) and conditions for their preparation for other $A^{III}B^{V}$ semiconductors, such as InSb, GaAs and GaSb.

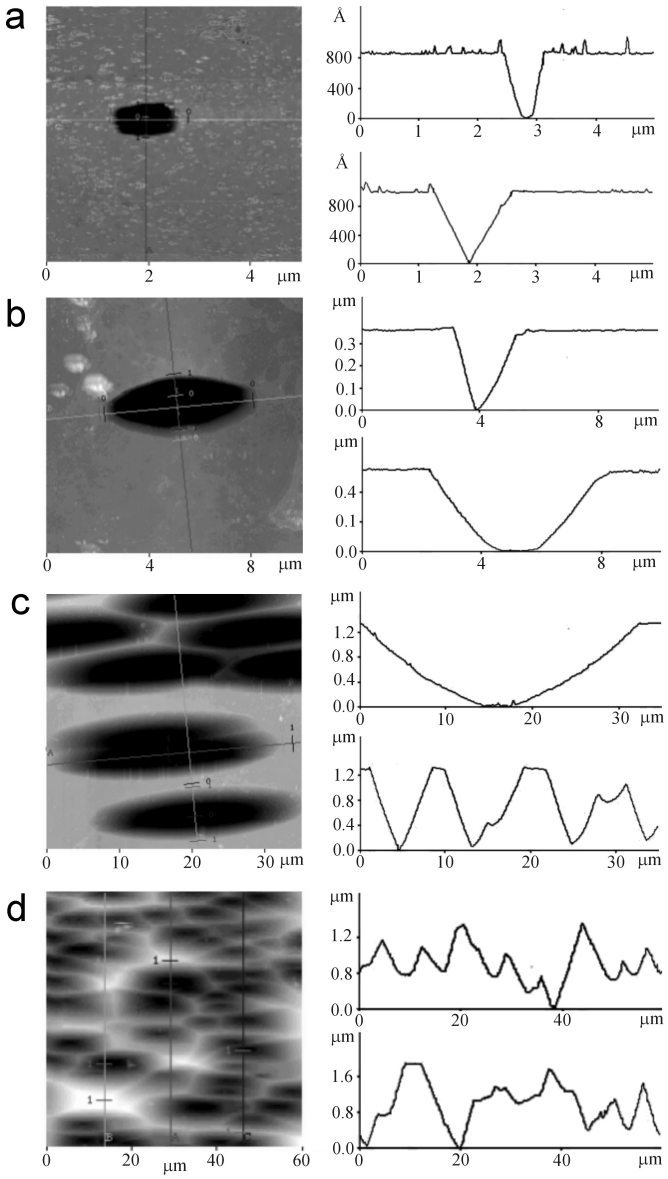

FIGURE 4. AFM images and geometrical parameters of GaP surface microreliefs after anisotropic etching in concentrated H_3PO_4 at 180 ˚ C for: (a) 1 min; (b) 2 min; (c) 4 min; (d) 5 min.

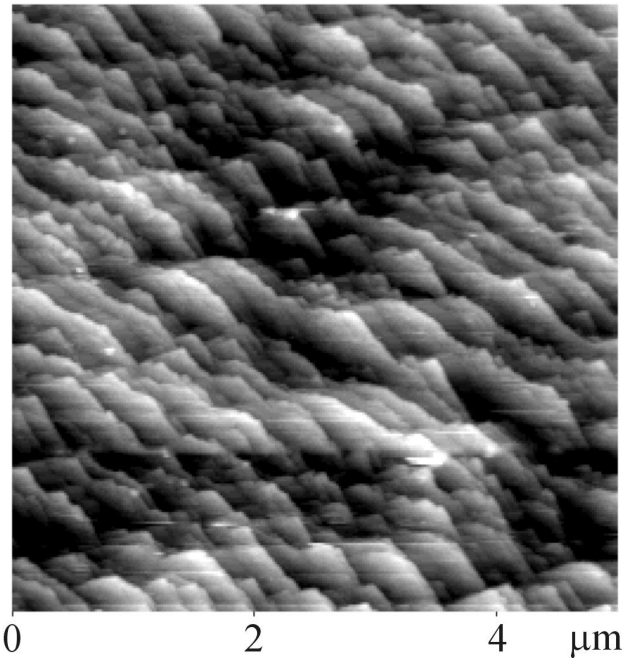

FIGURE 5. AFM image of GaP(100) surface microrelief obtained after two-step etching: concentrated HCl at 60 ˚ C for 1 min followed by concentrated H3PO4 at 60 ˚ C for 1 min.

The Fig. 6 shows groove-type microreliefes with U- and V-profile, formed after anisotropic etching in the mixture $1HCl{:}1H_2O_2{:}2H_2O$ for GaSb (a), after two-step etching in $5HNO_3{:}2HCl{:}1H_2O$ followed by $1HNO_3{:}1HCl$ for InSb (b), and after etching in $1H_3PO_4{:}1H_2O_2{:}1H_2O$ for GaAs (c). For all these textured surfaces the microrelief formation begins from some active centers (defects, impurities) finally forming a network structure of approximately parallel grooves oriented along [011] direction.

In the case of InSb such a microrelief morphology was obtained after anisotropic etching in $1HNO_3{:}1HCl$ mixture, but very similarly to the case of InP (Fe-doped), initially its quality was bad and the grooves side also had many roughnesses (Fig. 7a). To improve it, we again used the two-step etching procedure. The damaged surface layer of InSb was eliminated during the first step, by treating it in $5HNO_3{:}2HCl{:}1H_2O$ mixture. The resulting surface was textured in $1HNO_3{:}1HCl$ etchant, to produce the desired grooves. Figure 7 shows the difference in quality of the two InSb surfaces, textured through these different procedures. The temperature and time for $1HNO_3{:}1HCl$ treatment were equal in both cases.

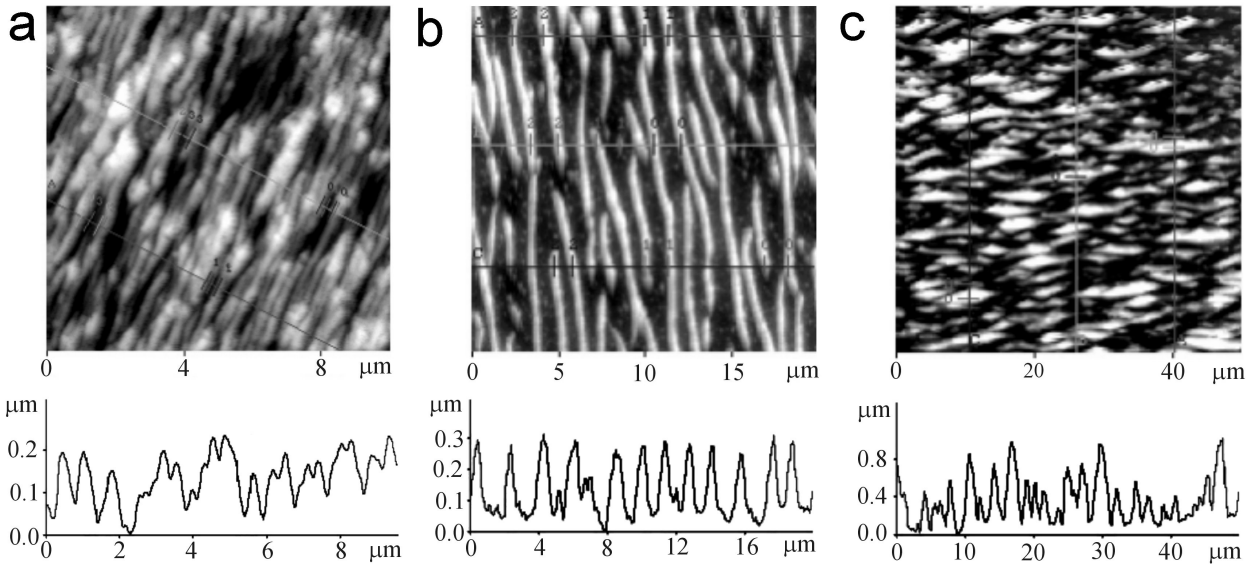

FIGURE 6. AFM images and geometrical parameters of surface microreliefs at: (a) GaSb etched in $1HCl{:}1H_2O_2{:}2H_2O$; (b) InSb etched in $5HNO_3{:}2HCl{:}1H_2O$, followed by $1HNO_3{:}1HCl$; (c) GaAs etched in $1H_3PO_4{:}1H_2O_2{:}1H_2O$.

Figure 8 presents experemental kinetic data for the dissolution of InP, GaP, InSb, GaAs and GaSb in the anisotropic etchants found to produce groove-type, grating-like periodic microreliefs. The kinetic data were obtained by the gravimetric method. The initial, induction period of the process was difficult to characterize by gravimetry due to slow dissolution of native oxide, and thus slow formation of a reaction interface. After this, the reaction proceeded much more vigorously. The corresponding parts of the kinetic curves have a steeper slope and reflects the microrelief formation, evolution and existence. Within this range, the microrelief dimensions (that is the grooves period) correlate linearly with the etching duration. In particular, for GaP the microrelief shown in Fig. 4d can be observed between 3 and 6 min; for InSb, between 0.5 and 1 min; for InP, between 2 and 10 min; for GaSb and GaAs, the periodic microrelief existed in the range of 1-2 min. In the case of InP treated with HCl, increasing the duration from 3 to 6 min caused an increase in period from 1.8 to 3.7 μm. In the case of GaSb, the period increased from 0.3 to 0.7 μm for 1 and 2 min, respectively. The period of InSb groove-type microrelief increased from 0.03 (for 0.3 min) to 0.087 μm (for 1 min).

A more detailed kinetic and thermodynamic characterization of the etching processes is a complicated task because of great difficulties in accurate evaluation of reaction order, as

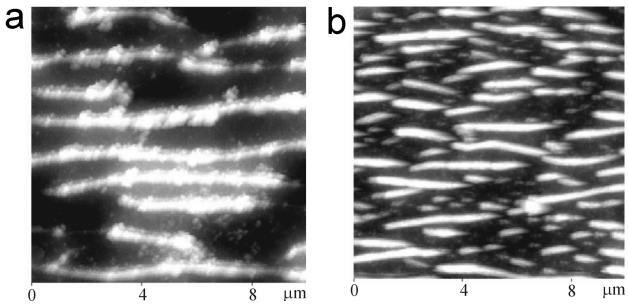

FIGURE 7. AFM images of InSb microrelief surfaces at: (a) $1HNO_3{:}1HCl$; (b) two-step etching in $5HNO_3{:}2HCl{:}1H_2O$ followed by $1HNO_3{:}1HCl$.

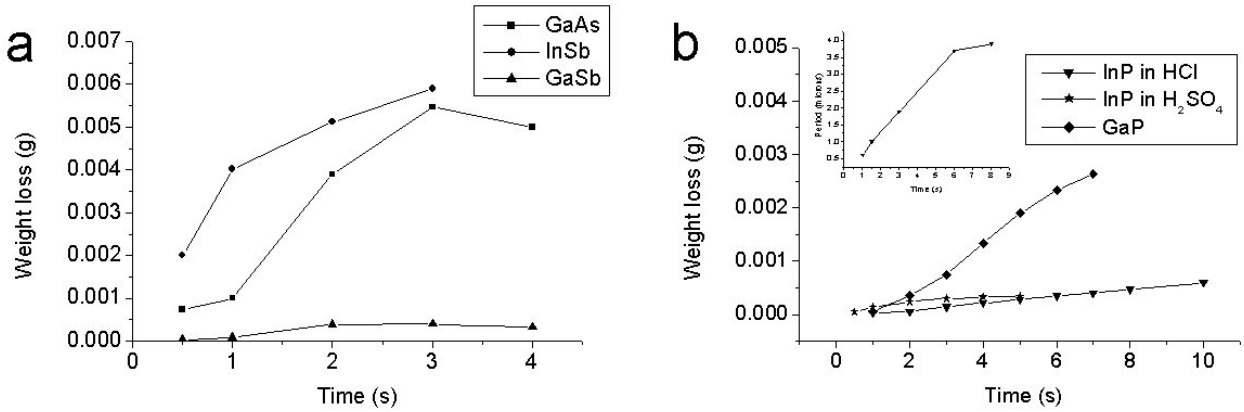

FIGURE 8. The experimental kinetic data (loss of sample mass during the etching) for semiconductors dissolution:(a) GaAs etched in $1H_3PO_4$:$1H_2O_2$:$1H_2O$, GaSb etched in HCl:H_2O_2:H_2O, InSb etched in $5HNO_3$:2HCl:$1H_2O$ followed by $1HNO_3$:1HCl; (b) InP etched in HCl , InP etched in H_2SO_4, GaP etched in H_3PO_4. Insert plot in (b) responds to the change in the grating period for InP surfaces during the etching in HCl.

TABLE I. Etchant composition for the microrelief preparation on InP(100), InSb(100), GaP(100), GaSb(100) and GaAs(100) surfaces by means of anisotropic etching, where K_v is the corresponding reaction rate for microrelief formation during dissolution reactions with specific temperature.

Semiconductor	Etchant composition	K_v (sec^{-1})	Temperature ($^\circ$C)
InSb	$5HNO_3$:2HCl:$1H_2O$ (step 1)		
	$1HNO_3$:1HCl (step 2)	2×10^{-3}	20
GaAs	$1H_3PO_4$:$1H_2O_2$:$1H_2O$	4.8×10^{-3}	80
GaP	H_3PO_4	8.8×10^{-4}	180
GaSb	HCl:$1H_2O_2$:$2H_2O$	2.6×10^{-5}	5
InP(S)	H_2SO_4	5.2×10^{-5}	120
InP(Fe)	$1HNO_3$:1HCl (step 1)		
	HCl (step 2)	2.6×10^{-6}	20

well as in obtaining kinetic data for the earliest etching stages. Nevertheless, for most semiconductors the etching process is usually considered to be pseudomonomolecular first-order reaction [13]. We assumed the above for the present cases of anisotropic etching, for the specific conditions when the microrelief formation and evolution is observed. Reaction rate constants K_v were calculated from the experimental kinetic data. Activation energies E_a were estimated for two different microrelief morphology in InP surfaces: grating-like microrelief (Fig.1a,b) and for the star-like figures (Fig. 3a). The E_a values are rather high, especially for InP etching in concentrated HCl (for HCl, E_a=25.68 kcal mol^{-1}; and for H_2SO_4, E_a=9.6 kcal mol^{-1}), thus indicating that both reactions occur in the kinetic region (transport-limited processes are characterized by lower E_a values, about 4-6 kcal mol^{-1} [13]). This means that the formation of grating-like microrelief is less favorable energetically. We can explain this phenomenon by high reaction capacity of the developed skeleton-type surface formed during the etching in H_2SO_4 (Fig. 3b), resulting in lowering the potential barrier. The kinetics for subsequent etching stages was not studied in detail, since under these conditions the microreliefs are smoothed, and the dissolution should be shifted to the transport-limited region.

4. Conclusions

Textured surfaces of diferent $A^{III}B^{V}$ semiconductors, namely InP(100) doped with Fe and S atoms, GaP(100), InSb(100),GaSb(100)andGaAs(100),werefabricated through spontaneous anisotropic chemical etching in strong acids and their mixtures. The results obtained are interesting from both phenomenological and practical points of view. Of all the microreliefs described in the present paper, the most interesting ones are the groove-type grating-like periodic microreliefs. Such a type of microreliefs can be obtained for almost all the representatives studied of $A^{III}B^{V}$ group of semiconductors. The data obtained on morphology evolution and kinetic behavior make it possible to control basic geometric parameters of the textured surfaces. Being considered as suitable to fabricate antireflection surfaces for solar cells, the preparation of similar textures reported elsewhere employed more complicated and expensive approaches, involving masking, photochemical and photoelectrochemical techniques and

requiring a special equipment. The simple chemical etching procedure proposed here extremely facilitates this task.

Acknowledgements

The authors thank V.A. Basiuk (Instituto de Ciencias Nucleares UNAM) for helpful comments on the manuscript, and J. Cañetas-Ortega (Instituto de Física UNAM) for assistance in SEM measurements. Also the authors would like to thank the Programa de Apoyo a Proyectos de Investigación e Innovación Tecnológica (grants DGAPA-IN106900 and -IN100402-3), and the Consejo Nacional de Ciencia y Tecnología (grant CONACyT-40399-Y) for the support during this study.

∗ Pseudonym of Elena Golovataya Dzhymbeeva.

1. H. Kawaguchi and G. Iwane, *J. Mater. Sci.* **16** (1981) 2449.
2. S. Adachi and H. Kawaguchi, *J. Electrochem. Soc.* **128** (1981) 1342.
3. S. Adachi, *J. Electrochem. Soc.* **129** (1982) 609.
4. D. Soltz, L. Cescato and F. Decker, *Sol. Energy mater. Sol. Cells.* **25** (1992) 179.
5. E.V. Basiuk, *Surface Coatings Technol.* **67** (1994) 51.
6. M. Kappelt and D. Bimberg, *J. Elechtochem. Soc.* **143** (1996) 3271.
7. N.L. Dmitruk, T.R. Barlas, and E.V. Basiuk, *Solar Energy Mater. Solar Cells* **31** (1993) 371.
8. Min-Gu Kang, Seung-Hoon Sa, Hyung-Ho Park, Kyung-Soo Suh, and Kyung-Hui Oh, *Thin Solid Films.* **308-309** (1997) 634.
9. P. Bonsch, D. Wullner, T. Schrimpf, A. Schlachetzki, and R. Lacmann, *J. Electrochem. Soc.* **145** (1998) 1273.
10. N.L. Dmitruk, O.Yu. Borkovskaya, and I.B. Mamontova, O.I. Mayeva and O.B. Yastrubchak, *Thin Solid Films* **364** (2000) 280.
11. N.L. Dmitruk, S.V. Mamykin, and O.V. Rengevych, *Appl. Surf. Sci.* **166** (2000) 97.
12. N.L. Dmitruk, E.V. Basiuk, G. Ya. Kolbasov, O.A. Yakubtsov, I.A. Molchanovskii and T.A. Taranets, Appl. Surf. Sci. **90** (1995) 489.
13. B.A. Irving, in P.J. Holmes (ed.), *The Electrochemistry of Semiconductors*. Primera Edición, Academic Press, New York, (1962) 256.
14. T. Ashley, T.M. Burke, G.J. Pryce, A.R. Adams, A. Andreev, B.N. Murdin, E.P. O'Reilly and C.R. Pidgeon, *Solid-State Electronics*, **47** (2003) 387.
15. D.L. Partin, J. Heremans and C.M. Thrush, *Sensors and Actuators A* **69** (1998) 39.
16. W.K. Wang, S.R. Qiu, B. Corbitt, S.T. Riggs and J.A. Yarmoff, *Surface Science*, **462** (2000) 211.